AMECJ

Research Article, Issue 4
Analytical Methods in Environmental Chemistry Journal
Journal home page: www.amecj.com/ir

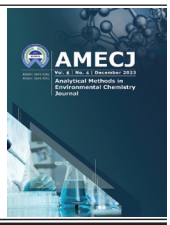

Removal of polypropylene nanoplastics from aqueous solution by biochar derived from Date palm fibers: Kinetics and isotherms studies

Mohammad Reza Rezaei Kahkha[a,*], Mahdi Rezaei Kahkha Zhaleh[b], Batool Rezaei Kahkha[a]

Maryam Khodadadi [c], and Mohsen Faghihi-Zarandi[d]

[a] *Faculty of Health, Zabol University of Medical Sciences, Zabol, Iran*
[b] *Student Research Committee, Isfahan University of Medical Sciences, Isfahan, Iran*
[c] *Departement of Environmental Health Engineering, School of Health, Medical Toxicology and Drug Abuse Research Center, Birjand University of Medical Sciences, Birjand, Iran*
[d] *Foreign Languages Department, Shahid Bahonar University of Kerman, Kerman, Iran*

ARTICLE INFO:

Received 25 Jul 2023
Revised form 11 Oct 2023
Accepted 7 Nov 2023
Available online 30 Dec 2023

Keywords:
Adsorption,
Activated carbon,
Polypropylene nanoplastics,
Date,
Kinetics,
Isotherm

ABSTRACT

In this work, activated carbon (AC) derived from powder of date palm fibers (DPF) was examined as an adsorbent for removing polypropylene nanoplastics (PPNPs) from aqueous solutions. The adsorbent was characterized using XRD, FT-IR, and SEM analyses. Affecting parameters on removal efficiency in a batch reactor, such as contact time, concentration of PPNPs and amount of adsorbent, were evaluated and optimized. Equilibrium and kinetic studies are performed to understand adsorption mechanisms. In the batch system, 30 mL of polypropylene suspension (5-40 mgL^{-1}) was added to Erlenmeyer flask. First, different amounts of AC adsorbent were added to the container, then microplastic was added to the reactor. The mixture was shaken on a shaker for four hours at 25°C. The flask was removed from the shaker, the concentration of PPNPs in the supernatant was measured, and a settling time of 30 min was obtained. A control suspension system without PPNPs nanoplastics (with biochar and without PPNPs) was also performed to evaluate carbon particle interference by turbidity measurements. Our results showed that kinetic data were consistent with the pseudo-second-order kinetic model. Equilibrium data for the adsorption of PPNPs on biochar represented by the Langmuir isotherm model is better than the Freundlich isotherm model.

1. Introduction

Microplastics are synthetic solid particles or polymer matrices with regular or irregular shapes, in sizes between 1 micrometre and 2 mm, with primary or secondary production origin and insoluble in water. Today, plastics are almost essential materials for human life. [1]The advantages of plastics, including long life, flexibility, resistance to light, excellent mechanical properties, resistance to atmospheric factors and long life, and low price, have led to their use in many cases to improve human life[1, 2]. Today, the global production of plastics is more than 361 million tons[3]. Microplastics can be classified based on their source. Primary microplastics are produced directly by humans, such as personal care products and cosmetic products[4]. Primary microplastics are

*Corresponding Author: Mohammad Reza Rezaei Kahkha
Email: m.r.rezaei.k@gmail.com
https://doi.org/10.24200/amecj.v6.i04.314

inevitably subjected to further degradation, which can change their size, morphology, color, density and surface functional groups. Secondary microplastics are obtained from the decomposition of larger pieces of plastic under chemical, physical and biological degradation in situ[5, 6]. Due to their widespread use, microplastics have spread everywhere and have been detected in freshwater, ocean, soil air, and polar regions [7]. The distribution of microplastics in aquatic environments is influenced by various factors such as size, shape, and type and the density of microplastics, as well as living organisms and chemicals in the water environment[8]. There are different ways for microplastics to enter environmental waters [9]. Studies have shown that the highest concentration of microplastics in fresh water is in glaciers and urban areas, followed by fresh water from rainwater and wetlands[10]. The concentration of microplastics has been reported from 900 to 2800 (ng m^{-3}) and from 1250 to 4650 nano gram per cubic meter, respectively, in Dongting Lake and Heng Lake[11, 12]. Minting and colleagues have reported the concentration of microplastics was 0 to 7 items per cubic meter in urban drinking water[13]. Another study showed that from 159 examined tap water samples from global sources, 81% were polluted with microplastics, with concentrations ranging from 0 to 61 pieces per litre, with an average of 5.45 pieces per litre [14]. Due to the importance of removing MPs from aquatic environments, many physical, chemical and biological methods have been proposed. Filtration, weight separation, electrified nanofiber membranes, coagulation and flocculation and sedimentation, advanced oxidation, membrane bioreactor, photocatalytic degradation and absorption are among the methods applied to remove MPs from water[15]. Among the mentioned methods, absorption is the most common, cheapest, fastest and oldest method used in water purification. The absorption method is environmentally friendly. Also, the process of doing it is easy, in addition, the absorbent can be used several times So far, adsorbents such as carbon nanotubes, graphene oxide, metal nanooxides, magnetic materials, coal, sand, activated carbon, aluminum chloride, silica gel, and other compounds such as clay, hydrogel, and sol gel have been used to remove microplastics from water. [16-18]. Also, polypropylene nanoplastics may be exist with other pollutants (VOCs and heavy metals) which must be analyzed based on nanotechnology before determination by GC or AAS methods. Recently, different carbon structures such as CNTs, active carbon, functionalized multi-walled carbon nanotubes, aminopropyl trimethoxysilane-phenanthrene carbaldehyde immobilized on graphene oxide, bimodal mesoporous silica nanoparticles, hydroxyethyl methylimidazolium tetrafluoroborate immobilized on MWCNTs, task-specific ionic liquids, Nanographene oxide modified phenyl methanethiol nanomagnetic composite, pyrrolic and pyridinic nitrogen doped porous, graphene nanostructure, and nano-palladium embedded on the mesoporous silica nanoparticles were used for removal VOCs and heavy metalsfrom water and air samples[19-28].

This research investigated the activated carbon obtained from date palm fibers for removing polypropylene pollutants from the water environment. The influencing variables on PPNPs absorption, including contact time, PPNPs initial concentration, and amount of adsorbent, were investigated and optimized.

2. Material and Methods

2.1. Reagents and Instruments

Polypropylene solution was obtained from Thermo Fisher Scientific-1862725 (Rheinach, Switzerland). Stock suspensions of 1.0 g L^{-1} were prepared from the original solution, which contained 10 g L^{-1} of PPNPs microplastic particles and diluted with ultrapure water (Milli Q water, Millipore, Switzerland). Before use, PPNPs stock suspension was sonicated for 15 min with a sonication bath (Bransonic ultra cleaner, Branson 5510 model, Switzerland). The stock solution was stored in a dark place at a constant temperature of 4 °C and used for further experiments.

2.2. Preparation of adsorbent

Activated carbon was prepared from the remaining dates collected from Zabol villages in eastern Iran. For the preparation of biochar, The date palm fibers biomass are placed in a ceramic tube in a horizontal

furnace for 3 hours at a temperature of 400 degrees Celsius under a nitrogen flow at a speed of 5 cm^3 per second. Before activation, the particles are crushed and sieved. 10 g of charcoal were mixed with 10 g of KOH and stirred for four hours. Then, the obtained charcoal was placed in the oven for 48 hours at 150 °C . After drying, biochar was transferred to the furnace under nitrogen flow at 700 °C for 4 hours. Then, the activated charcoal was washed with HCl and distilled water, respectively, until it reached neutral pH, and then the absorbent was dried in an oven at 80 °C for 24 hours[29].

2.3. *Characterization of adsorbents*

An X-ray diffractometer (XRD, ALMELO, Netherlands) was utilized to get the XRD patterns of the date fibers structure. The SEM instrument (SEM, QUANTA 400F) depicted the surface morphology images. SEM images assisted in revealing the changes in the surface morphology that occurred due to adsorbent synthesizing or due to the adsorption process. FT-IR, Perkin Elmer Mattson 1000 (USA), was utilized to determine the functional group's presence on the date powder and its significance in adsorption. The analysis of FT-IR was conducted within the wavenumber region of 500–4000 cm^{-1}. The StablCal stabilized formazin turbidity standards was use by the turbidimeter The concentration of PS nanoplastics before and after batch adsorption experiments was determined by measuring the supernatant suspension's turbidity at different times. Before analysis, the instrument was calibrated with StablCal solutions from Hach, and the light scattered by the particles was measured in Formazine Nephelometric Unit (FNU).

2.4. *Bach adsorption experiment*

The experiments were conducted in a 150 mL Erlenmeyer flask containing 30 mL polypropylene suspension with an initial concentration from 5.0 to 40 mg L^{-1}. Before adding microplastic to the reactor, different amounts of adsorbent were added to the container.(Fig.1) The obtained suspension was shaken on a shaker at a speed of 100 rpm for 240 minutes at room temperature. The flask was removed from the shaker, and the concentration of PPNPs nanoplastics in the supernatant was measured. Before analysis, all samples were left to settle for another 30 min to minimize interference of carbon particles. A settling time of 30 min was determined experimentally. A control suspension system without PPNPs nanoplastics (with biochar and without PPNPs) was also performed to evaluate carbon particle interference by turbidity measurements. These data were used to calculate the concentration of PPNPs nanoplastics in the supernatant suspension. The flask contents were shaken for a particular time with a speed of 150 rpm.

The adsorbed amount of the PPNPs, q_e (mg g^{-1}), was computed using Equation 1.

$$q_e = \frac{(C_i - C_{eq})V}{m} \qquad \text{(Eq.1)}$$

Where q_e (mg g^{-1}) is the equilibrium adsorbed amount, and C_i (mg L^{-1}) is the initial concentration. C_{eq} (mg L^{-1}) is the equilibrium concentration, and V (L) is the

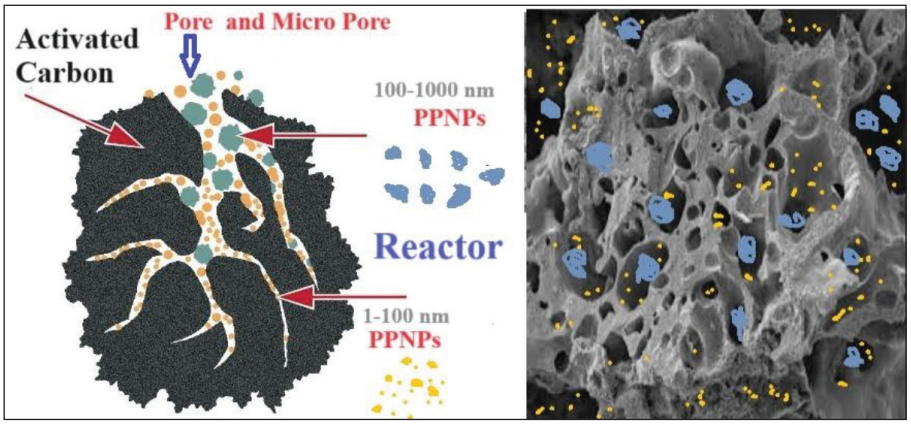

Fig.1. Adsorption polypropylene nanoplastics by activated carbon in reactor

volume of solution that contains mass (g) of adsorbent. Kinetic studies were performed to determine the adsorption rate of the PPNPs onto biochar in a separate experiment. Isotherms of the Langmuir and Freundlich models were applied to comprehend the adsorption mechanism (Eq.2). The adsorption capacity was calculated using Equation 3. The rate of the adsorption of the PPNPs was modelled using pseudo-first-order and pseudo-second-order kinetics. The linear equation of pseudo-first-order kinetic was used in Equation 4. The linear equation of the pseudo-second-order model is shown in Equation 5. The linear equation of the Langmuir isotherm model is expressed by Equation 6. The parameter R_L was calculated according to Equation 7, which can be used to expect the efficiency of the adsorbent. Based on the value of the R_L parameter, the process is irreversible if R_L is equal to zero, favourable if R_L is less than 1, linear if R_L is equal to 1 and unfavourable if R_L is greater than 1. The equation 8 was used for the Freundlich isotherm model.

Mass of PPNPs adsorbed = $(C_i - C_f) \times V$ (Eq.2)

$$\text{Adsorption capacity} = \frac{M_{adsorbate}}{M_{adsorbent}} \quad \text{(Eq.3)}$$

As Equation 3: C_i: Initial concentration of PPNPs in (mg L^{-1}), C_f: Final concentration of PPNPs in (mg L^{-1}), V: volume of the solution in (L), M_{PPNPs}: Mass of PPNPs in (g), $M_{adsorbent}$: Mass of adsorbent in (g)

$$\log(q_e - q_t) = \log(q_e) - \left(\frac{k_1}{2.303}\right) t \quad \text{(Eq.4)}$$

Where k_1 is the rate constant of the pseudo-first-order adsorption process (min^{-1}), q_e is the equilibrium adsorbed amount of material per unit mass of adsorbent (mg g^{-1}), q_t is the equilibrium adsorbed amount of material per unit mass of adsorbent at time t (mg g^{-1}).

$$\frac{t}{q_t} = \frac{1}{k_2 q_e^2} - \frac{1}{q_e} t \quad \text{(Eq.5)}$$

Where, k_2 is the rate constant of the pseudo-second-order adsorption process (g mg^{-1} min^{-1}), q_e is the equilibrium adsorbed amount of material per unit mass of adsorbent (mg g^{-1}), and q_t is the equilibrium amount of material adsorbed per unit mass at time t (mg g^{-1}). The rate constant value of k_2 was obtained using the slope and intercept from the plot of t/q_t versus t.

$$\frac{C_e}{q_e} = \frac{1}{k_L q_m} + \frac{C_e}{q_m} \quad \text{(Eq.6)}$$

Where q_e is the equilibrium adsorbed amount of the material (mg g^{-1}), q_m is the maximum capacity of adsorption (mg g^{-1}), K_L is the Langmuir isotherm constant related to the energy of adsorption and is used to determine the affinity of the adsorbate to the adsorbent surface. C_e is the equilibrium material concentration in the solution (mg L^{-1}). The values of K_L and q_m constants were obtained using the slope and the intercept from the linear plot of C_e/q_e versus C_e.

$$R_L = \frac{1}{1 + k_L C_i} \quad \text{(Eq.7)}$$

Where K_L is the Langmuir isotherm constant determined in Equation 6, Ci is the initial concentration of the adsorbate.

$$\log q_e = \log K_f + \frac{1}{n} \log C_e \quad \text{(Eq.8)}$$

Where q_e is the equilibrium concentration of the solid phase material per gram of adsorbent (mg g^{-1}), C_e is the equilibrium concentration of the material in the bulk phase (mg L^{-1}), K_f is the Freundlich isotherm constant (mg g^{-1}), and n is the intensity of adsorption. The values of K_f and n were obtained using the slope and the plot intercept between log q_e and log C_e.

3. Results and discussion

3.1. Characterization of Adsorbent

FT-IR, SEM, and XRD were employed to characterize the adsorption process of the PPMPs (R, Y, and E) onto biochar.

3.1.1. FTIR analysis

Based on the FT-IR analysis of the raw date fibers, peaks observed in the spectra indicated several

functional groups at the surface, which serve as active sites for adsorption on the adsorbent surface. Figure 2 shows many bands at 3300.23 (related to O–H stretching vibration), 3010 (related to O–H stretching vibration), 1738.09 cm^{-1}(related to stretching vibration of C=O of carboxylic groups), 1710.09 (related to stretching vibration of C=O of carboxylic groups), 900.42(related to C=C, the C-H bond, and O-H in the plane deformation), and 528.89 (related to C-H deformation vibration and CH_2 rocking vibration –C–N– and –C–C– stretching) cm^{-1}. Also, SEM images and XRD of the morphology of biochar are shown in Figures 3 and 4.

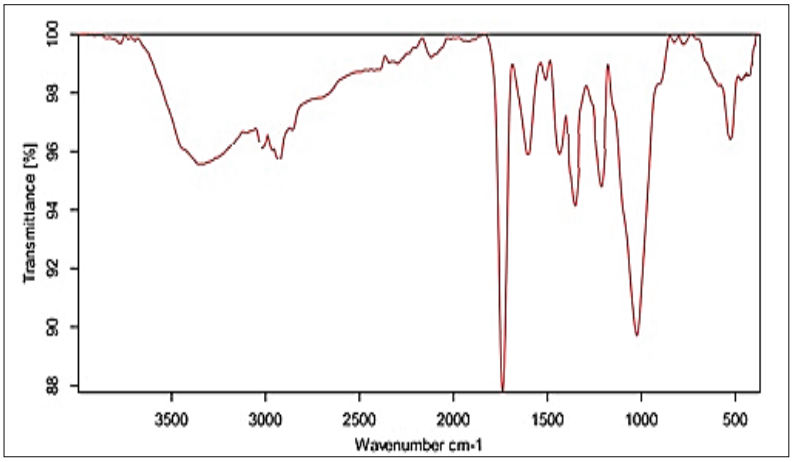

Fig. 2. FT-IR analysis of biochar derived from palm date fibers powder

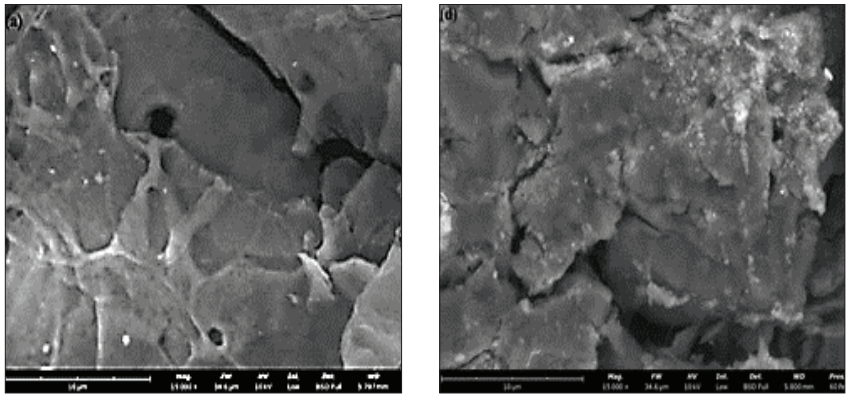

Fig. 3. SEM analysis of (a) date palm fibers biochar, (b) PPNPs on biochar

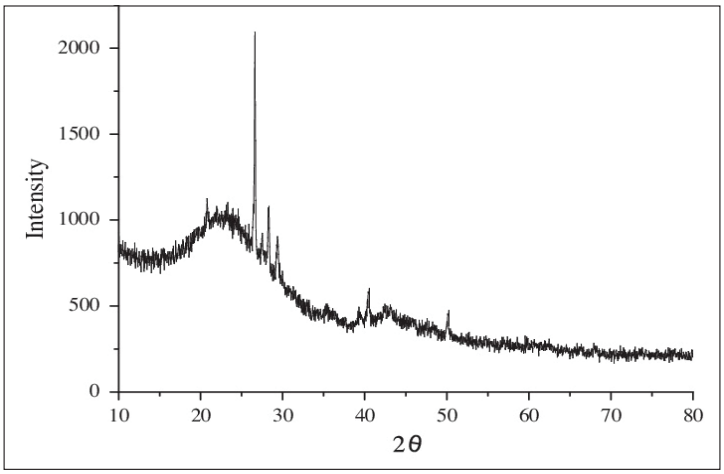

Fig. 4. XRD pattern of date palm fibers biochar

3.2. Batch adsorption

3.2.1. Influence of amount of adsorbent

The amount of adsorbent is a critical factor in the adsorption process. The variation in the adsorbent dosage impacts the adsorption of PPNPs onto biochar. Figure 5 shows the aschematic adsorption process. The removal efficiency and the adsorption capacity were investigated. The study was conducted using an adsorbent dosage of 10 to 100 mg. The optimal conditions used in this study were shaking at 150 rpm for 60 min at a concentration of 50 mg L^{-1}, a temperature of 25 ± 1 °C, and a pH of 7.0. As shown in Figure 6, the adsorption of the PPNPs was significantly increased up to 80 mg. Furthermore, while increasing the amount of biochar, the percent removal efficiency was increased, gradually decreasing the adsorption capacity.

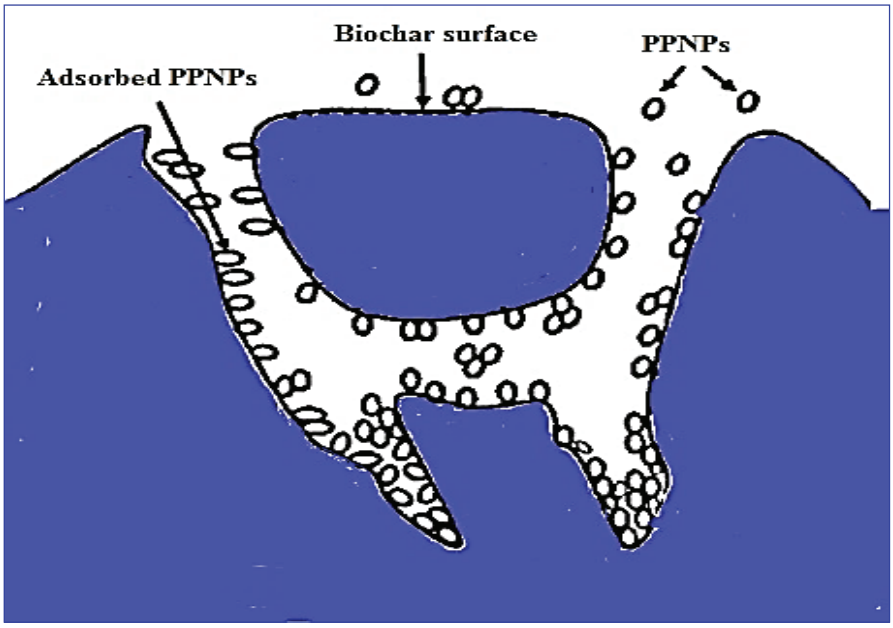

Fig. 5. Schematic adsorption process of PPNPs on biochar

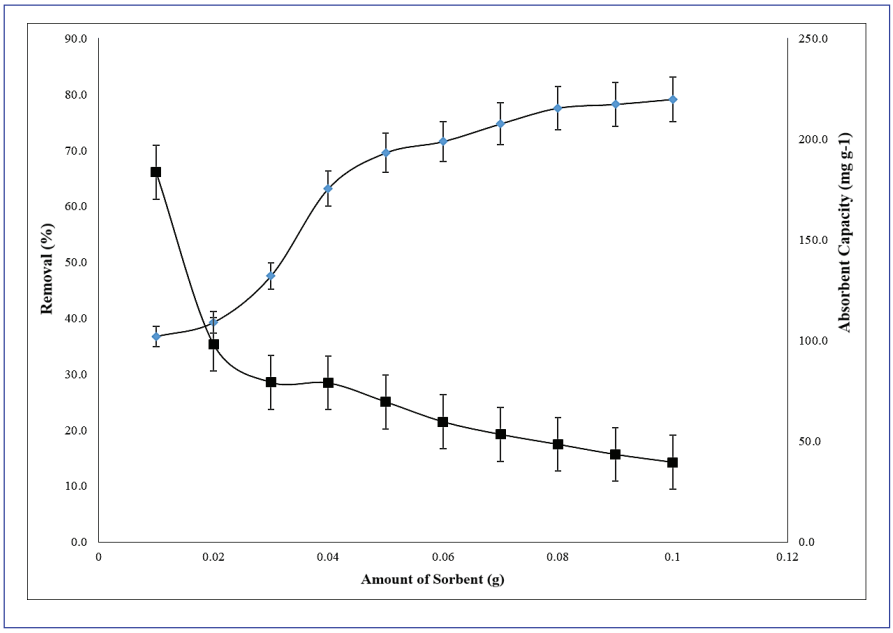

Fig. 6. Influence of adsorbent dosage on the adsorption of PPNPs on biochar[adsorbent dosage = 0.01-0.1 g, initial concentrations = 50 mg. L^{-1}; pH = 7.0, and contact time = 60 min, and T= 25 ±1°C]

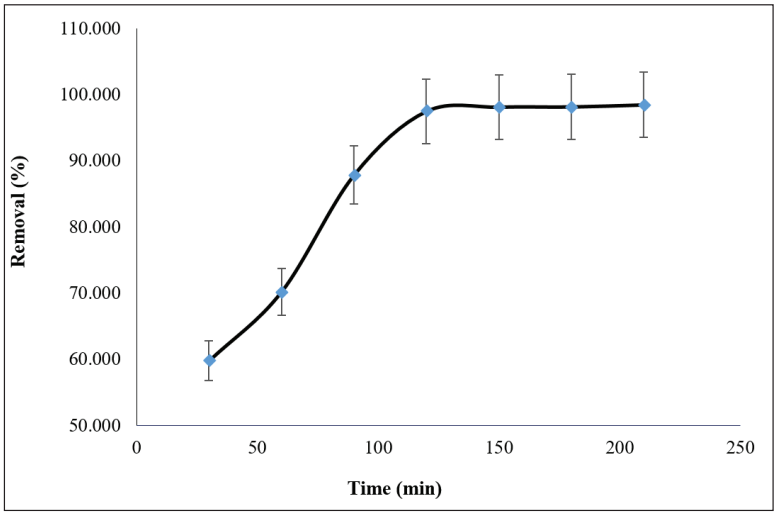

Fig. 7. Effect of contact time on the adsorption of PPNPs [time = 20-210 min., initial concentrations = 50 mg. L^{-1}; pH = 7.0, and T = 25 ±1°C]

3.2.2. Influence contact time

The impact of contact time on the removal efficiency of PPNPs by adsorbent was investigated. The optimal conditions used in this study were, a mass of adsorbent 80 mg of biochar, a temperature of 25 ± 1 °C, and a pH of 7.0. The removal percentages for the PPNPs increased significantly in the early stages. This behavior is related to the abundance of accessible active sites on the adsorbent. The results showed that the PPNPs needed 120 minutes to reach equilibrium which are shown in Figure 7.

3.2.3. Effect of PPNPs concentration

The variation in the initial concentration of the PPNPs impacts the removal percentage by biochar. The initial concentrations of 25 -150 mg L^{-1} were studied. The optimal conditions used in this study were obtained at 150 rpm shaking for 60 min, a mass of adsorbent 80 mg for PPNPs, a temperature of 25 ± 1 °C, and a pH of 7.0. The results of the PPNPs concentration on removal are shown in Figure 8. The results showed a significant increase at the beginning of the adsorption process. The maximum percent removal was investigated at a concentration of 50 mg L^{-1} for the PPNPs. Over time, the saturation of active biochar sites increased, resulting in a slight decrease in the adsorption capacity of biochar[30].

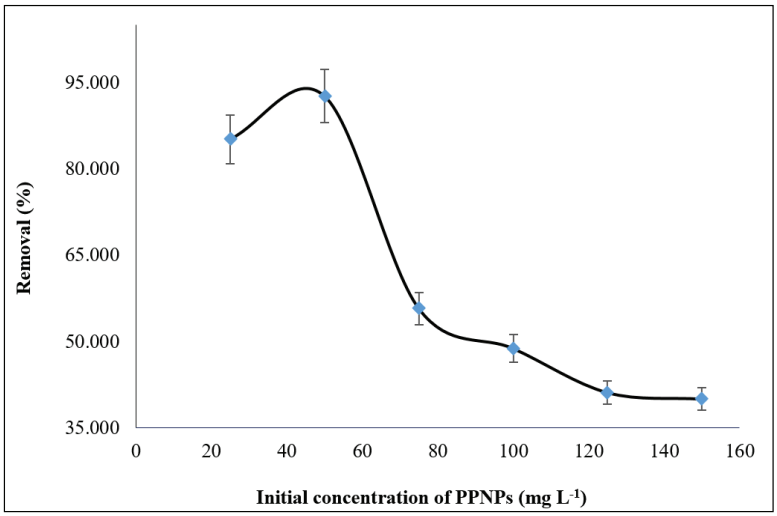

Fig. 8. Effect of initial concentration of PPNPs on the removal efficiency.[pH = 7.0, rpm = 150, and Temperature = 25 ±1°C]

3.2.4. Adsorption kinetic studies

Kinetics is an important step to determine the adsorption mechanism and to understand the biosorption steps that affect the processing speed. As a result of kinetic studies, it is possible to determine the rate of adsorption, and the retention time required for the used adsorbent to perform pollutant removal can be determined. The rate of adsorption is an important parameter in the selection of the most suitable adsorbent in the adsorption process. In determining the adsorption rate and rate constant, pseudo-first-order and pseudo-second-order kinetic models such as particle diffusion are applied to the xperimental data, and the kinetic model that best fits the experimental data is determined. Therefore, adsorption kinetic studies of PPNPs onto biochar were investigated using pseudo-first-order and pseudo-second-order kinetics. The results are summarized in Table 1 and Figure 9. R^2 values determined the kinetic model that best fits the adsorption of PPNPs onto biochar. Considering the reported R^2 values, the adsorption of PPNPs onto biochar followed pseudo-second-order kinetics. It was observed that the experimental data showed a high agreement to pseudo-second-order kinetic models (R^2> 0.989 in all conditions examined for this models), When the model data obtained were evaluated considering all of the experiments.

3.2.5. Adsorption isotherms

Langmuir and Freundlich's isotherms were used to illustrate the mechanism of the adsorption process. The Langmuir and Freundlich isotherms constants for the adsorption of PPNPs on biochar were calculated (Table 2). It was found that the adsorption of PPNPs is a favorable process according to the obtained results for Langmuir isotherm.

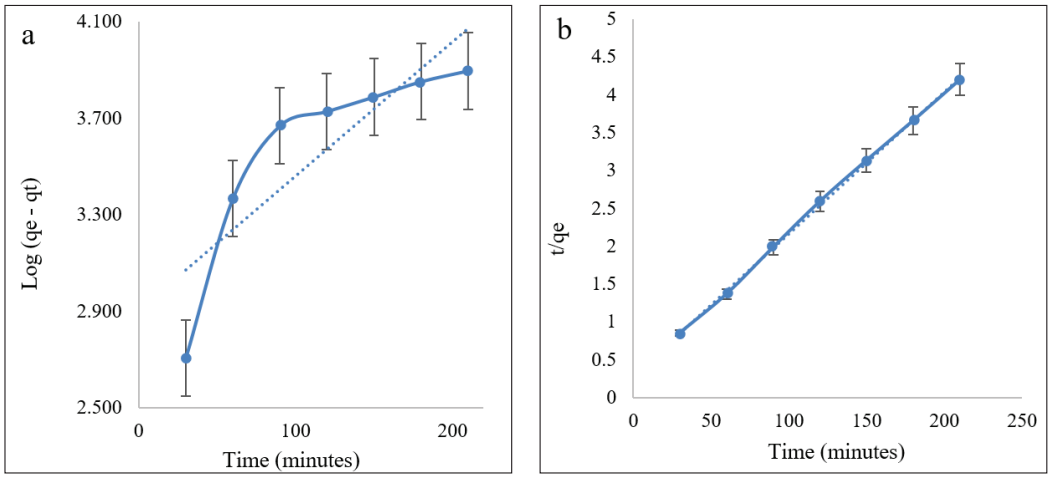

Fig. 9. Kinetic studies of the adsorption of PPNPs on biochar.
a: Psuedo First order **b:** Psuedo second order

Table 1. Adsorption of PPNPs by pseudo-first-order and pseudo-second-order kinetics

	First order kinetics		Second order kinetics	
	R^2	K_1 (min^{-1})	R^2	K_1 ($g.mg^{-1}min^{-1}$)
PPNPs	0.8512	$4.598X10^{-3}$	0.9899	$1.65X10^{-2}$

Table 2. The Langmuir and Freundlich isotherms constants of PPNPs adsorption biochar

	Langmuir			Freundlich		
	R_L^2	R_L	K_L	R_F^2	K_F	n
PPMPs	0.9019	0.1123	0.4521	0.9803	11.9652	2.7456

4. Conclusion

The adsorption mechanism of PPNPs on biochar derived from date fibers as an adsorbent was investigated. The results obtained from the characterization techniques (FT-IR, XRD, and SEM) confirm the adsorbent characterization. The optimal conditions for removing PPNPs were the amount of adsorbent 80 mg, contact time of 120 min, and initial concentration of 50 mg L^{-1} for the PPNPs. The isotherm data could be obtained according to the Langmuir model. The kinetic data of the PPNPs are modelled by the pseudo-second-order, revealing that the nature of the kinetic adsorption is chemical. The present study shows biochar derived from date fibers to be an effective adsorbent for removing PPNPs from aqueous solutions.

5. Aknowledgement

The authors thanks to Zabol University of Medical Sciences, Isfahan University of Medical Sciences, Birjand University of Medical Sciences, and Shahid Bahonar University of Kerman, Iran.

6. References

[1] Y. Yu, W.Y. Mo, T. Luukkonen, Adsorption behaviour and interaction of organic micropollutants with nano and microplastics–a review, Sci. Total Environ., 797 (2021) 149140. https://doi.org/10.1016/j.scitotenv.2021.149140

[2] F. Wang, M. Zhang, W. Sha, Y. Wang, H. Hao, Y. Dou, Y. Li, Sorption behavior and mechanisms of organic contaminants to nano and microplastics, Molecules, 25 (2020) 1827. https://doi.org/10.3390/molecules25081827

[3] W. J. Shim, S.H. Hong, S.E. Eo, Identification methods in microplastic analysis: a review, Anal. methods, 9 (2017) 1384-1391. https://doi.org/10.1039/C6AY02558G

[4] K. Zhang, A.H. Hamidian, A. Tubić, Y. Zhang, J.K. Fang, C. Wu, P.K. Lam, Understanding plastic degradation and microplastic formation in the environment: A review, Environ. Pollut., 274 (2021) 116554. https://doi.org/10.1016/j.envpol.2021.116554

[5] A.A. Koelmans, P.E. Redondo-Hasselerharm, N.H.M. Nor, V.N. de Ruijter, S.M. Mintenig, M. Kooi, Risk assessment of microplastic particles, Nat. Rev. Mater., 7 (2022) 138-152. https://doi.org/10.1038/s41578-021-00411-y

[6] F. Stock, C. Kochleus, B. Bänsch-Baltruschat, N. Brennholt, G. Reifferscheid, Sampling techniques and preparation methods for microplastic analyses in the aquatic environment–A review, TrAC Trends Anal. Chem., 113 (2019) 84-92.https://doi.org/10.1016/j.trac.2019.01.014

[7] M. Shahraki, M.R. Rezaei Kahkha, J. Piri, A. Sharafi, M. Kaykhaii, Microplastics in atmospheric dust samples of Sistan: sources and distribution, J. Environ. Health Sci. Eng., 20 (2022) 931-936. https://doi.org/10.1007/s40201-022-00833-y

[8] J.A.I. do Sul, M.F. Costa, The present and future of microplastic pollution in the marine environment, Environ. pollut., 185 (2014) 352-364. https://doi.org/10.1016/j.envpol.2013.10.036

[9] A.L. Andrady, Microplastics in the marine environment, Marine Pollut. Bull., 62 (2011) 1596-1605. https://doi.org/10.1016/j.marpolbul.2011.05.030

[10] Y. Zhang, T. Gao, S. Kang, S. Allen, X. Luo, D. Allen, Microplastics in glaciers of the Tibetan Plateau: evidence for the long-range transport of microplastics, Sci. Total Environ., 758 (2021) 143634. https://doi.org/10.1016/j.scitotenv.2020.143634

[11] W. Wang, W. Yuan, Y. Chen, J. Wang, Microplastics in surface waters of dongting lake and hong lake, China, Sci. Total Environ., 633 (2018) 539-545. https://doi.org/10.1016/j.scitotenv.2018.03.211.

[12] C. Jiang, L. Yin, X. Wen, C. Du, L. Wu, Y. Long, Y. Liu, Y. Ma, Q. Yin, Z. Zhou, Microplastics in sediment and surface water of west Dongting Lake and south Dongting Lake: abundance, source and composition, Int. J. Environ. Res. Public Health, 15

(2018) 2164. https://doi.org/10.3390/ijerph15102164

[13] S. Mintenig, M. Löder, S. Primpke, G. Gerdts, Low numbers of microplastics detected in drinking water from ground water sources, Sci. Total Environ., 648 (2019) 631-635. https://doi.org/10.1016/j.scitotenv.2018.08.178

[14] M. Kosuth, S.A. Mason, E.V. Wattenberg, Anthropogenic contamination of tap water, beer, and sea salt, PLOS One, 13 (2018) e0194970. https://doi.org/10.1371/journal.pone.0194970

[15] M. Padervand, E. Lichtfouse, D. Robert, C. Wang, Removal of microplastics from the environment. A review, Environ. Chem. Lett., 18 (2020) 807-828. https://doi.org/10.1007/s10311-020-00983-1

[16] W. Liu, J. Zhang, H. Liu, X. Guo, X. Zhang, X. Yao, Z. Cao, T. Zhang, A review of the removal of microplastics in global wastewater treatment plants: Characteristics and mechanisms, Environ. Int., 146 (2021) 106277. https://doi.org/10.1016/j.envint.2020.106277

[17] M. Shen, B. Song, Y. Zhu, G. Zeng, Y. Zhang, Y. Yang, X. Wen, M. Chen, H. Yi, Removal of microplastics via drinking water treatment: Current knowledge and future directions, Chemosphere, 251 (2020) 126612. https://doi.org/10.1016/j.chemosphere.2020.126612

[18] R. Ahmed, A.K. Hamid, S.A. Krebsbach, J. He, D. Wang, Critical review of microplastics removal from the environment, Chemosphere, 293 (2022) 133557. https://doi.org/10.1016/j.chemosphere.2022.133557

[19] F. Golbabaei, A. Vahid, A. Faghihi Zarandi, A novel nano-palladium embedded on the mesoporous silica nanoparticles for mercury vapor removal from air by the gas field separation consolidation process, Appl. Nanosci., 12 (2022) 1667-1682. https://doi.org/10.1007/s13204-022-02366-0

[20] M. Habibnia, A. Rashidi, A.F. Zarandi, M.D. Mobarake, Simultaneously speciation of mercury in water, human blood and food samples based on pyrrolic and pyridinic nitrogen doped porous, graphene nanostructure, Food Chem., 403 (2023) 134394. https://doi.org/10.1016/j.foodchem.2022.134394

[21] M.K. Abbasabadi, F. Hosseini, Nanographene oxide modified phenyl methanethiol nanomagnetic composite for rapid separation of aluminum in wastewaters, foods, and vegetable samples by microwave dispersive magnetic micro solid-phase extraction, Food Chem., 347 (2021)129042. https://doi.org/10.1016/j.foodchem.2021.129042

[22] N. Esmaeili, J. Rakhtshah, Ultrasound assisted-dispersive-modification solid-phase extraction using task-specific ionic liquid immobilized on multiwall carbon nanotubes for speciation and determination mercury in water samples, Microchem. J., 154 (2020) 104632. https://doi.org/10.1016/j.microc.2020.104632

[23] R. Ashouri, Dynamic and static removal of benzene from air based on task-specific ionic liquid coated on MWCNTs by sorbent tube-headspace solid-phase extraction procedure, Int. J. Environ. Sci. Technol., 18 (2021) 2377-2390. https://doi.org/10.1007/s13762-020-02995-4

[24] J. Rakhtshah, A rapid extraction of toxic styrene from water and wastewater samples based on hydroxyethyl methylimidazolium tetrafluoroborate immobilized on MWCNTs by ultra-assisted dispersive cyclic conjugation-micro-solid phase extraction, Microchem. J., 170 (2021) 106759. https://doi.org/10.1016/j.microc.2021.106759

[25] P. Paydar, A novel method based on functionalized bimodal mesoporous silica nanoparticles for efficient removal of lead aerosols pollution from air by solid-liquid gas-phase extraction, J. Environ. Health Sci. Eng., 18 (2020) 177–188. https://doi.org/10.1007/s40201-020-00450-7

[26] S. Teimoori, An immobilization of aminopropyl trimethoxysilane-phenanthrene carbaldehyde on graphene oxide for toluene extraction and separation in water samples, Chemosphere, 316 (2023) 137800. https://doi.org/10.1016/j.chemosphere.2023.137800

[27] S. Teimoori, A.H. Hassani, M. Panahi, N. Mansouri, Rapid extraction of BTEX in water and milk samples based on functionalized multi-walled carbon nanotubes by dispersive homogenized-micro-solid phase extraction, Food Chem., 421 (2023) 136229. https://doi.org/10.1016/j.foodchem.2023.136229

[28] S. Teimoori, A.H. Hassani, New extraction of toluene from water samples based on nano-carbon structure before determination by gas chromatography, Int. J. Environ. Sci. Technol., 20 (2023) 6589–6608. https://doi.org/10.1007/s13762-023-04906-9

[29] A.H. Tahir, A.H.M. Al-Obaidy, F.H. Mohammed, Biochar from date palm waste, production, characteristics and use in the treatment of pollutants: A Review, IOP Conf. Ser. Mater. Sci. Eng., 373 (2020) 012171. https://doi.org/10.1088/1757-899X/737/1/012171

[30] R. Mao, M. Lang, X. Yu, R. Wu, X. Yang, X. Guo, Aging mechanism of microplastics with UV irradiation and its effects on the adsorption of heavy metals, J. Hazard. Mater., 393 (2020) 122515. https://doi.org/10.1016/j.jhazmat.2020.122515